Climate
of the Past
Discussions

Holocene atmospheric iodine evolution over the North Atlantic

Juan Pablo Corella[1], Niccolo Maffezzoli[2,3], Carlos Alberto Cuevas[1], Paul Vallelonga[2], Andrea Spolaor[3], Giulio Cozzi[3], Juliane Müller[4], Bo Vinther[2], Carlo Barbante[3,5], Helle Astrid Kjær[2], Ross Edwards[6,7] and Alfonso Saiz-Lopez[1*]

5   [1]Department of Atmospheric Chemistry and Climate, Institute of Physical Chemistry Rocasolano, CSIC, Serrano 119, 28006 Madrid, Spain

[2]Centre for Ice and Climate, Niels Bohr Institute, University of Copenhagen, Juliane Maries vej 30, Copenhagen Ø 2100, Denmark

[3]Institute for the Dynamics of Environmental Processes, IDPA-CNR, Via Torino 155, 30170 Mestre, Italy

10 [4]Alfred Wegener Institute, Helmholtz Center for Polar and Marine Research, Am Alten Hafen 26, 27568 Bremerhaven, Germany

[5]Ca´Foscari University of Venice, Department of Environmental Sciences, Informatics and Statistics, Via Torino 155, 30170 Venice Mestre, Italy

[6]Physics and Astronomy, Curtin University of Technology, Kent St, Bentley WA 6102, Australia

15 [7]Department of Civil and Environmental Engineering, UW-Madison, Madison, WI 53706, USA

Correspondence to: A. Saiz-Lopez (a.saiz@csic.es)

Abstract. Atmospheric iodine chemistry has a large influence on oxidizing capacity and associated radiative impacts in the troposphere. However, information on the evolution of atmospheric iodine levels is restricted to the Industrial Period while its long-term natural variability remains unknown. The current levels of iodine in the atmosphere are controlled by anthropogenic
20   ozone deposition to the ocean surface. Here, using high-resolution ice core measurements from coastal eastern Greenland (ReCAP ice core), we report the first record of atmospheric iodine variability during the Holocene (last 11,700 years). Surprisingly, our results reveal that the highest iodine concentrations in the record, found during the Holocene Thermal Maximum (~11,500-5,500 years before -present). These high iodine levels could be driven by ocean primary productivity resulting in an Early Holocene "Biological Iodine Explosion". The iodine trend during this past warm period is a useful
25   observational constraint on projections of future changes in Arctic atmospheric composition and climate resulting from global warming.

1 Introduction

The Holocene (last 11,7 kyr BP) has sustained the growth and development of modern society. The integration of
30   environmental proxies from different natural archives allows a detailed understanding of Holocene climate (*Mayewski et al.*, 2004). Nevertheless, there is surprisingly little systematic knowledge about atmospheric chemistry during this period, which

is a key factor to understand the background of natural variability underlying anthropogenic climate change. Global atmospheric models have recently shown the significant contribution of halogen chemistry to the oxidizing capacity of the atmosphere and associated radiative impacts (*Hossaini et al.*, 2015; *Saiz-Lopez et al.*, 2012, 2014; *Sherwen et al.*, 2016, 2017).

35   Reactive halogens containing chlorine, bromine and iodine atoms cause ozone depletion through efficient catalytic cycles (*Saiz-Lopez and von Glasow*, 2012, *Simpson et al., 2015*). In particular, atmospheric reactive iodine has a global contribution of up to 27% of the total rate of ozone loss in the marine boundary layer and upper troposphere (*Saiz-Lopez et al.*, 2014). Iodine-mediated ozone depletion negatively contributes to the longwave radiative flux in the troposphere (*Hossaini et al.*, 2015; *Saiz-Lopez et al.*, 2012; *Sherwen et al., 2017*). Reactive iodine could also be involved in new atmospheric particle

40   formation (*Allan et al.*, 2015; *Roscoe et al.*, 2015; S*ipilä et al.*, 2016), which has been suggested to have potential climatic implications in the troposphere.

The origins and cycling of iodine in the global atmosphere involves ocean emissions from inorganic (hypoiodous acid (HOI) and molecular iodine (I_2)) and organic sources (CH_3I, CH_2I_2, CH_2ICl and CH_2IBr)). Globally, the main source of present-day atmospheric iodine is the inorganic emission of HOI and I_2 from the ocean surface as a product of the reaction of iodide

45   with deposited ozone (*Carpenter et al.*, 2013; *MacDonald et al.*, 2014; *Prados-Roman et al.*, 2015). Biota in the marine environment are known to produce alkyl iodides, which are a primary source of reactive iodine due to their short photolysis lifetimes (from minutes to several days) (*Saiz-Lopez et al.*, 2012). In polar regions, another important source of reactive iodine is the biogenic production of HOI and I^- from algae underneath the sea-ice (in equilibrium with I_2 and H_2O), and its subsequent diffusion through brine channels to the overlying atmosphere (*Saiz-Lopez et al.*, 2015). Other proposed mechanisms for iodine

50   reaction in ice include the production of I_2 and tri-iodide (I_3^-) through the photo-oxidation of iodide (*Kim et al.*, 2016), and the heterogeneous photo-reduction of iodate (*Gálvez et al.*, 2016). The recycling of iodine on ice/snow surfaces represents an offset change in partitioning ultimately increasing the effective atmospheric lifetime of iodine against deposition (*Saiz-Lopez et al.*, 2014). Particle-bound iodine compounds related to terrestrial biogenic material and mineral dust might also contribute to the total atmospheric iodine concentrations (*Spolaor et al.*, 2013). Sea spray aerosols (ssa) expelled from the ocean surface

55   during wave breaking also incorporate iodine in their structure, which can be subsequently released to the gas phase mainly due to the photolysis of the diatomic ICl and IBr species recycled by heterogeneous reactions over ssa (McFiggans et al., 2000; *Saiz-Lopez et al.*, 2014).

The polar ice sheets continuously archive atmospheric composition, and ice core records can be used to reconstruct atmospheric iodine deposition at centennial to millennial time-scales. ice core iodine reconstructions are limited to two coastal

60   sites: Law Dome (east Antarctica) (*Vallelonga et al.*, 2017) and Severnaya Zemlya (Russian Arctic) (*Spoloar et al.*, 2016). Iodine variability recorded at these sites is strongly affected by regional sea-ice dynamics since sea-ice bioproductivity is thought to be one of the main sources of Antarctic and Arctic iodine (*Saiz-Lopez et al.*, 2015). Unfortunately, the iodine records extracted from Law Dome and Severnaya Zemlya barely span the past few decades, thus preventing the assessment of millennial-scale atmospheric iodine variability and its source emission mechanisms. The only iodine record beyond the

65   Industrial Period available to date is restricted to Talos Dome (coastal Antarctica) (*Spolaor et al.*, 2013), which provides a

reconstruction of iodine variability for the last two glacial cycles. This record does not allow a Holocene reconstruction of iodine variability and related environmental drivers due to the low temporal resolution of the record (mean resolution >2 kyrs/sample) and the lack of iodine data during the last four millennia (*Spolaor et al.*, 2013).

70 The ReCAP ice core (from the Renland ice cap, eastern Greenland, Fig. 1) constitutes the only Greenland ice core with a complete Holocene climate stratigraphy largely undisturbed by glaciological "brittle ice" effects (*Vinther et al.*, 2009). The Renland ice cap is an ideal location for investigating ocean trace gas emissions since air masses feeding this region are mostly influenced by the North Atlantic Ocean from 50ºN to the Fram Strait (*Maffezzoli et al.*, 2018). A recent study of the upper 130 m in the ReCAP ice core (CE 1750-2011) shows, for the first time, a threefold increase in the Arctic and the North Atlantic iodine concentration during the last six decades. This increase is mainly driven by anthropogenic ozone pollution and

75 enhanced sub-ice phytoplankton production associated with the recent thinning of Arctic sea ice (*Cuevas et al.*, 2018) This threefold increase has also been recorded in an alpine ice core (Col du Dome ice core), which likely records iodine emissions from the Mediterranean Sea (*Legrand et al.*, 2018). The recent increase in anthropogenic ozone in the troposphere and its subsequent deposition on the ocean surface favours the ozone reaction with iodide ions, accelerating the release of HOI and I_2 to the atmosphere (*Prados-Roman et al.*, 2015, *Cuevas et al.,* 2018; *Legrand et al.,* 2018).

80 However, the environmental drivers of atmospheric iodine levels at millennial time-scales, prior to anthropogenic influences are still unknown. Here, we show the first complete, high-resolution reconstruction of atmospheric iodine during the Holocene. We combine the ReCAP ice core measurements with other marine paleoceanographic archives to investigate the main environmental mechanisms driving millennial-scale natural atmospheric iodine variability during the Holocene.

2 Data and Methods

85 **2.1 Study site.**

The Renland ice cap is located on a high mountain plateau in Scoresby Sund fjord system (coastal eastern Greenland) isolated from the main Greenland ice sheet. The 584 m long ReCAP (Renland ice CAP) ice core (71°18'18"N, 26°43'24"W; 2315 m a.s.l.) was drilled to bedrock in May-June 2015 using the Danish Hans Tausen intermediate drill system. The core is located just 2 km from the site of the original Renland ice core, drilled in 1988 to a depth of 324 m, from which a site accumulation

90 rate of 50 cm ice equivalent/yr was determined (Hansson et al., 1994).

The ReCAP ice core record covers the last 120 kyr BP. This study focuses on the upper 535 meters that constitute the Holocene (last 11.7 kyr BP). The Holocene age-depth model is based on annual layer counting for the interval (CE 2015 - 4 kyr BP, where BP signifies 'before CE 1950'); combined with a modified Dansgaard-Johnsen ice flow model (*Dansgaard and Johnsen*, 1969) constrained to well-dated age markers from 4 to 11.7 kyr BP. The annual layer counting was conducted using

95 the StratiCounter algorithm (*Winstrup et al.*, 2012) constrained by volcanic eruption markers and synchronized to the GICC05 Greenland Ice Core Chronology framework (*Vinther et al.*, 2006).

2.2 Ice core sampling and geochemical analyses.

Each one of the ice core samples devoted to the geochemical analyses (n=1035) was collected by integrating 55 cm of melted

100   ice from a Continuous Flow Analysis (CFA) system (University of Copenhagen). The meltwater was collected in polyethylene

tubes and subsequently refrozen and stored shielded from light until analyses. Some of the samples were sent to the

Environmental Analytical Chemistry laboratory (IDPA-CNR) of the University of Venice, while others were sent to the Curtin

University of Technology (Perth, Australia). Iodine and sodium concentrations were measured by i) Sector Field Inductively

Coupled Plasma Sector Field Mass Spectroscopy (ICP-SFMS, Element XR, Thermo Fisher, Germany) in Australia (defined

105   CUT system) and by ii) Inductively Collision Reaction Cell-Inductively Coupled Plasma-Mass Spectrometry (CRC-ICP-MS,

Agilent 7500cx, Agilent, California, USA) in Italy (defined IDPA-CNR system). For the Italian measurements, the operational

methodology is the same as in Spolaor et al., (2013) (*Spolaor et al.*, 2013). Iodine (^{127}I) was determined at low mass resolution

with stability of instrumental signal evaluated by the continuous monitoring of ^{129}Xe. The sample line was thoroughly cleaned

using 2% nitric acid and UPW between each analysis. Instrumental errors for iodine and sodium concentrations were 10%.

110   Respective sodium and iodine detection limits were 1 ppb and 0.005 ppb for the Venice CRC-ICP-MS and 1.1 ppb and 0.002

ppb for the Perth ICP-SFMS. 140 samples were analysed at both institutions for intercomparison in order to investigate

differences between the analytical techniques and laboratories (Fig. S1). The ratio of the iodine measurements carried out in

the two institutions average $\rho = 0.95 \pm 0.01$ highlighting the strong correlation between the measurements at both institutions.

The iodine and sodium measurement temporal resolution ranged from sub-annual in the upper metres to decadal to

115   centennial during the Mid- to Early Holocene (average resolution of 0.08 samples/yr) according to the RECAP ice core age-

depth model and sampling resolution. The ice core iodine annual depositional fluxes were calculated according to the equation:

$$\text{Iflux} = [\text{I}] \ x \ \text{AR}$$

where (I) and AR represent the iodine concentrations and reconstructed annual accumulation rates (Fig. S2), respectively.

Pearson coefficients during the main Holocene climatic phases (i.e.; Holocene Thermal Maximum, Neoglacial, Late Holocene

120   and Great Acceleration) were calculated to evaluate the statistical correlation between geochemical variables -i.e. (I), (Na) and

(Ca)- analyzed in ReCAP ice cores.

2.3 Atmospheric Chemistry modelling.

THAMO (Tropospheric HAlogen chemistry Model) is a 1-D chemistry transport model with 200 stacked boxes at a vertical

resolution of 5 m (total height 1 km). The model includes a complete scheme for iodine, bromine, chlorine, O_3, NO_x and HO_x

125   tropospheric chemistry, and is constrained with typical measured values of other chemical species in the MBL (*Saiz-Lopez et

al.*, 2008). The model THAMO has been applied in this study to characterize interactive halogen photochemistry and the

production of tropospheric reactive iodine during the present day and two different scenarios during the Holocene. The model

is initialized at midnight to build up all species before the sunrise, when the sunlight starts all the photolytic processes. Three

different scenarios have been investigated in which different preconditioning factors have been applied according to published

130   paleoenvironmental reconstructions (Table S2) and the MERRA reanalysis dataset (*Rienecker et al.*, 2011). Inorganic iodine

emission fluxes were calculated according to laboratory-based flux parametrization (*Carpenter et al., 2013*) with mean values ranging from 0.0037 to 0.0039 mol m^{-2} kyrs^{-1} for the HTM and the Neoglacial period respectively. These values were calculated using 10 ppbv of tropospheric ozone in the atmosphere before Industrialization (*Volz and Kley*, 1988) and 35 ppbv during the Great Acceleration (*Cooper et al.*, 2014).

135 **3 Results**

Holocene iodine concentrations (I) and fluxes (I$_{flux}$, i.e. iodine annual depositional rates from the atmosphere to the ice surface) in the ice core range from 0.06 ng g^{-1} to below the detection limit (mean 0.02 ng g^{-1}) and from 35 to 0.01 $\square$g m^{-2} yr^{-1} (mean 8.1 $\square$g m^{-2} yr^{-1}) respectively (Fig. 2, Fig. S2). Iodine concentrations from ice core records in Greenland may suffer from significant remobilization processes, particularly in areas with low annual snow accumulation rates (*Legrand et al.*, 2018).

140 However, losses of volatile iodine species would be strongly reduced in areas with high annual snow accumulation rates such as the Renland peninsula (annual snow accumulation rates ˜ 0.5 kg m^{-2}, yr^{-1}; Fig. S2). Thus, Holocene iodine variability may respond to the interplay of different inorganic and biogenic emission sources. Laboratory studies indicate that current global inorganic iodine emissions are maintained by the reaction between iodide (I^{-}) ions with atmospheric ozone deposited to the sea surface (*Carpenter et al.*, 2013; *MacDonald et al.*, 2014). Lower inorganic iodine emissions to the atmosphere have been

145 hypothesized (*Prados-Roman et al.*, 2015), on account of the commensurately lower level of atmospheric ozone (about 10 ppb) occurring before the onset of industrialization (*Volz and Kley*, 1988). According to the THAMO model, ocean inorganic iodine emissions were low ~10.1 ± 0.6 nmol m^{-2} d^{-1} throughout Holocene climatic periods (Table S1), contrasting with the four-fold (I) variability recorded in the ReCAP record during the last 11.7 kyrs BP (Fig. 2). This suggests that the Holocene high atmospheric iodine levels cannot be attributed to ozone-driven inorganic iodine emission sources.

150

3.1 Iodine levels during the Holocene Thermal Maximum (~11.5-5.5 kyr BP).

The iodine concentrations measured in the ReCAP ice core show the highest values during the Holocene Thermal Maximum (HTM), peaking at ~10 kyr BP and remaining at the same levels until ~5.5 kyr BP (mean (I) of 0.036 ng g^{-1}) (Fig. 2 and S2). Similarly, the iodine fluxes remained high throughout the HTM (mean I fluxes = 14.2 ug m^{-2} yr^{-1}). This period exhibited warm

155 surface water conditions (1.6±0.8°C higher than present (*Kaufman et al.*, 2004)) and salinity increases in the Arctic (*Briner et al.*, 2016; *Solignac et al.*, 2006) as a result of high summer insolation (Fig. 2).

Several micropaleontological and organic geochemical biomarker records suggest a decrease in sea-ice coverage throughout the HTM (*Cabedo-Sanz et al.*, 2016; *Müller et al.*, 2012; *Ślubowska-Woldengen et al.*, 2008; *Vare et al.*, 2009; *Werner et al.*, 2016; *Xiao et al.*, 2017). The paleoenvironmental reconstructions carried out in multiple settings from the

160 northern North Atlantic and the Arctic Ocean (Fig. 1, Table S2) also indicate higher primary productivity in this region during the Early Holocene (Fig. 2). The subpolar species *T. quinqueloba*, indicative of warm and saline Atlantic Water advection (*Volkmann*, 2000), as well as of nutrient-rich subsurface waters (*Werner et al.*, 2016), was dominant in the northern North Atlantic and Nordic seas during the HTM, as far north as the Fram Strait (*Werner et al.*, 2013; *Werner et al.*, 2016). Higher

concentrations of dinosterol and brassicasterol, respective biomarkers of dinoflagellates and diatoms (*Volkman et al.*, 1998),
165   also indicate higher primary productivity in the subpolar North Atlantic during the HTM (*Kolling et al.*, 2017; *Müller et al.*,
2012; *Werner et al.*, 2016). The increase in terrestrial sediment delivery and nutrient supply derived from Arctic glacier melting
and coastal erosion during the Early Holocene (*Solomina et al.*, 2015; *Wegner et al.*, 2015) may have promoted higher marine
productivity in Arctic shelf and coastal areas. An increase in planktonic foraminifera depositional fluxes and higher bio-
induced calcium carbonate precipitation in the Northern North Atlantic and the Nordic seas (*Telesiński et al.*, 2015; *Werner et*
170   *al.*, 2013) (Fig. 2, Table S2) provide further evidence of enhanced primary productivity. These biological species, including
phytoplankton and macro- and micro-algae, accumulate iodine to concentrations of up to 10^3-10^6 greater than in seawater and
produce iodine compounds in the ocean (*Saiz-Lopez et al.*, 2012). The increase in primary productivity would lead to an
enhancement of the biological iodine production in the ocean, followed by its release to the atmosphere resulting in "Biological
Iodine Explosion" (BIE). Maximum summertime solar irradiance in the Arctic during the HTM (Fig. 2) would also slightly
175   increase the algae oxidative stress increasing the iodine effusion rates from the surface ocean (*Saiz-Lopez et al.*, 2012; 2015).
Additionally, higher sea surface temperatures (SST) during the HTM would favor the sea-air phase transfer of volatiles (i.e.
iodine compounds) produced at the ocean surface. Greater primary productivity in the reduced summertime sea ice-covered
Nordic Seas drives two biological changes resulting in enhanced iodine release from the ocean surface: firstly, enhanced
emission of iodocarbons from the open ocean directly to the atmosphere and secondly the enhanced production of iodine (I_2)
180   by sea-ice phytoplankton colonies and its release to the atmosphere through brine channels and ice cracks formed in the thinner
HTM seasonal sea ice (*Saiz-Lopez et al.*, 2015). Inorganic iodine emissions (10.7 nmol m^{-2} d^{-1}) would only account for 25%
of the total HTM iodine emissions, as inferred by the THAMO model (Table S1). No significant correlation is found between
iodine and sodium or calcium ice core concentrations (Table S3), suggesting that iodine variability during the HTM is not to
be attributed either to atmospheric transport of ssa or to dust-related particle-bound iodine. We therefore conclude that ocean
185   biogenic iodine production and emission operating on millennial timescales (~11.5-5.5 kyr BP) played the dominant role (up
to 75% of iodine emissions, Table S1) in the observed HTM iodine record.

3.2 Iodine levels during the Neoglacial Period (~5.5-3.4 kyr BP)

An abrupt decrease in iodine levels occurs during the Neoglacial period (Fig. 2 and S1), a time interval characterized by a
190   general cooling of the Arctic and North Atlantic regions (*Jennings et al.*, 2002; *Koç et al.*, 1993; *Nesje and Dahl*, 1993). Iodine
concentrations and fluxes are at their lowest levels in the entire sequence with mean values of 0.008 ng g^{-1} and 3.9 ug m^{-2} yr^{-1},
respectively. A significant correlation exists between iodine and sodium (Table S3) suggesting an influence of ssa variability
on iodine concentrations during the Neoglacial period.

The HTM ended quite abruptly *c*. 5.5 kyr BP when global sea level reached its modern value and a hence intensified
195   sea-ice production in the Kara and Laptev Seas resulted in a perennial sea-ice cover in the central Arctic Ocean and enhanced
sea ice export into the North Atlantic (*Bauch et al.*, 2001; *Cronin et al.*, 2010; *Telesiński et al.*, 2015; *Werner et al.*, 2013).
Increased sea-ice coverage and/or reduced summer sea-ice break up is also reported for the Greenland-Norwegian Sea and

eastern Fram Strait after c. 5.5 kyr BP (*Koç et al.*, 1993; *Müller et al.*, 2012; *Telesinski et al.*, 2014; *Telesiński et al.*, 2014; *Werner et al.*, 2013). Recent sea-ice reconstructions from the North Iceland Shelf show that the HTM was followed by a

200   pronounced re-advance of sea ice at about 6 kyr BP (*Cabedo-Sanz and Belt*, 2016; *Xiao et al.*, 2017), when SST started to decrease (*Kristjánsdóttir et al.*, 2017). Increased sea ice ultimately reduces atmospheric iodine emission through a number of direct and indirect processes involving reduced marine primary production (Fig. 2; Table S2 and references therein). Thicker sea ice would reduce the amount of sunlight reaching algae colonies underneath sea ice, thus reducing the amount of seawater iodine compounds (*Saiz-Lopez et al.*, 2015). Thicker and/or more extensive sea ice would also impede the iodine diffusion

205   through ice and further release of I_2 to the overlying atmosphere (*Saiz-Lopez et al.*, 2015). Both these combined processes likely contributed to the observed ice core iodine minimum during the Neoglacial period. Our modelling results indicate that inorganic iodine emissions (10.1 nmol m^{-2} d^{-1}) account for most of the low atmospheric iodine concentration during the Neoglacial period (Table S1).

210   **3.3 Iodine levels during the Late Holocene (~3.4 kyr BP- Present)**

Iodine levels vary widely during the Late Holocene with concentration and fluxes ranging from 0.064 ng g^{-1} to below the detection limit (mean (I) of 0.017 ng g^{-1}) and from 35 to 0.015 ug m^{-2} yr^{-1} (mean 8 ug m^{-2} yr^{-1}), respectively. Iodine concentrations slightly increased at 3.4 kyr BP and remained fairly constant until 0.8 kyr BP (mean (I) and I fluxes of 0.014 and 6.34 ug m^{-2} yr^{-1} respectively) (Fig 2 and S2).

215   Arctic sea-ice extent progressively increased during the Late Holocene as recorded in mid- and high-latitude Arctic locations (e.g. (*Cabedo-Sanz et al.*, 2016; *Werner et al.*, 2013; *Werner et al.*, 2016)) (Fig. 2, Table S1). Sea-ice reconstructions from the East Greenland shelf, however, reveal a slightly reduced but stable sea-ice cover during the last 3 kyr consistent with increasing phytoplankton growth and marine productivity (*Kolling et al.*, 2017) (Fig. S4). This trend is consistent with moderately increasing iodine levels recorded in the ReCAP ice core over the last 3 kyr (Figs. 2, S3 and S4).

220   Ice core iodine concentration and fluxes increased by 50% during the last eight centuries reaching mean values of ~0.021 ng g^{-1} and 8.9 ug m^{-2} yr^{-1} respectively at the onset of the Industrial Period (CE 1750-1850). The iodine time series in this part of the record reveals a higher frequency, which is in part due to a reduced ice compression towards the surface and thus an increased temporal resolution of the samples. Model results indicate that organic and inorganic iodine emissions contributed equally to the total iodine released to the atmosphere during the Late Holocene (Table S1). Phytoplankton

225   productivity in the Eastern Greenland shelf varied significantly during the Little Ice Age (LIA, CE 1400-1850), even reaching the highest values since the HTM (*Kolling et al.*, 2017) (Fig. 2). Sea ice re-advances and/or intensified sea ice export from the Arctic Ocean along the Greenland shelf and North of Iceland during the LIA (*Cabedo-Sanz et al.*, 2016; *Kolling et al.*, 2017) and a 10% decrease in solar irradiance since the Early Holocene (Fig. 2; Table S2) likely explained the atmospheric iodine levels being lower in the late Holocene with respect to the higher levels recorded during the HTM.

Climate
of the Past
Discussions

4 Discussion and Conclusions

Iodine levels in the ReCAP ice core have tripled since the onset of the Great Acceleration (1950 CE- Present) (*Cuevas et al.*, 2018). This very recent atmospheric iodine increase is explained by the rise in anthropogenic ozone pollution since the mid-20th century (*Cooper et al.*, 2014; *Cuevas et al.*, 2018; *Legrand et al.,* 2018) since oceanic inorganic emissions of HOI and I_2 depend on surface ozone concentrations (*Carpenter et al.*, 2013; *MacDonald et al.*, 2014; *Prados-Roman et al.*, 2015). A recent global modelling study has shown that inorganic iodine emissions from the oceans constitute ~75% of present-day total atmospheric iodine (*Prados-Roman et al.*, 2015). In the absence of human disturbances to iodine biogeochemical cycling during the HTM, the remarkably high iodine levels recorded in the ReCAP ice core can only be explained by natural drivers influencing iodine emissions to the atmosphere. Our results show that at the onset of the Holocene, enhanced ocean primary production coupled with maxima in solar irradiance and open water conditions in the Arctic ocean and in the Nordic Seas (*Bauch et al.*, 2001; *Cronin et al.*, 2010; *Müller et al.*, 2012; *M M Telesiński et al.*, 2014; *Werner et al.*, 2013; 2016) controlled iodine emissions to the atmosphere (Fig. 3) resulting in a four millennia-long period of high atmospheric iodine concentrations. The decrease in iodine levels observed at the onset of the Neoglacial period coincide with environmental modifications in the Arctic, primarily the advance of sea ice and the reduction of marine primary production (Fig. 2, Table S1 and references therein).

The fluctuations in atmospheric iodine levels recorded in the ReCAP ice core most likely resulted in significant long-term environmental impacts that ultimately affected the Holocene atmospheric chemistry and associated radiative impacts. The Early Holocene high iodine emissions might have led to enhanced aerosol concentrations in the Arctic atmosphere since atmospheric iodine promotes the formation of new ultrafine aerosol particles in coastal (*Mahajan et al.*, 2011; *O'dowd et al.*, 2002; *Sipilä et al.*, 2016) and polar regions (*Allan et al.*, 2015; *Roscoe et al.*, 2015). Furthermore, higher iodine levels have the potential to considerably accelerate atmospheric tropospheric ozone loss by up to 14 % and 27 % in the global marine boundary layer and upper troposphere, respectively (*Saiz-Lopez et al.*, 2014). Tropospheric ozone loss ultimately affects the oxidative capacity of the atmosphere and ozone radiative forcing which can in turn impact on climate by cooling the global troposphere by approximate -0.1 W m^2 (*Hossaini et al.*, 2015; *Saiz-Lopez et al.*, 2012; *Sherwen et al.,* 2017). The high variability of marine iodine fluxes to the continents could also have implications for land ecosystems during the Holocene since iodine is a key trace element in animal and human endocrine systems *(De Benoist et al., 2004)*.

Our results highlight that the increase in atmospheric iodine levels since 1950 CE is neither acute nor unusual in the context of long-term (i.e. millennial-scale) iodine variability. Therefore, the high levels of atmospheric iodine which occurred during the early Holocene may serve as an analogue for future atmospheric composition and climate conditions. This is particularly relevant to the Arctic, for which ice-free summertime conditions have been forecast to occur by 2050 CE (*Overland and Wang*, 2013).

Climate
of the Past
Discussions

Open Access

EGU

5 Data availability

The ice core and model data that support the findings of this study will be made available on the PANGAEA and NOAA
265 paleoclimate public databases after publication.

6 Author contribution

A.S.L., P.V. and A.S. designed the research. J.P.C., N.M., H.A.K., C.A.C., G.C., C.B., P.V. and R.E. collected and measured
the samples, and analyzed the resulting data. B.V. constructed the chronology. J.M. supplied primary production and sea-ice
270 coverage data. All authors interpreted the results. J.P.C. and A.S.L. wrote the manuscript with contributions from all authors.

7 Competing interests

The authors declare no competing interests.

8 Acknowledgments

9 References

Allan, J. D., Williams, P. I., Najera, J., Whitehead, J. D., Flynn, M. J., Taylor, J. W., Liu, D., Darbyshire, E.,
285 Carpenter, L. J., Chance, R., Andrews, S. J., Hackenberg, S. C., and McFiggans, G.: Iodine observed in new particle
formation events in the Arctic atmosphere during ACCACIA, *Atmos. Chem. Phys.*, 15, 5599-5609, 2015
Bauch, H. A., Erlenkeuser, H., Spielhagen, R. F., Struck, U. J., Matthiessen, J., Thiede, J. and Heinemeier, J., A
multiproxy reconstruction of the evolution of deep and surface waters in the subarctic Nordic seas over the last 30,000 yr,
Quaternary Science Reviews, *20*(4), 659-678, 2001
290 Briner, J. P., McKay, N. P., Axford, Y., Bennike, O., Bradley, R. S., de Vernal, A., Fisher, D., Francus, P., Fréchette,
B. and Gajewski K., Holocene climate change in Arctic Canada and Greenland, *Quaternary Science Reviews*, *147*, 340-364.
2016
Cabedo-Sanz, P., and Belt, S. T., Seasonal sea ice variability in eastern Fram Strait over the last 2000 years, *arktos*,
2(1), 22., 2016
295 Cabedo-Sanz, P., Belt, S. T., Jennings, A. E., Andrews, J. T. and Geirsdóttir, Á., Variability in drift ice export from
the Arctic Ocean to the North Icelandic Shelf over the last 8000 years: a multi-proxy evaluation, *Quaternary Science Reviews*,
146, 99-115, 2016.
Carpenter, L. MacDonald, J., S. M. Shaw, M. D. Kumar, R. Saunders, R. W. Parthipan, R. Wilson, J. and Plane J.
M., Atmospheric iodine levels influenced by sea surface emissions of inorganic iodine, *Nature Geoscience*, *6*(2), 108, 2013.

300   Cooper, O. R., Parrish, D. Ziemke, J.. Cupeiro, M Galbally, I. Gilge, S. Horowitz, L. Jensen, N. Lamarque, J.-F. and Naik, V., Global distribution and trends of tropospheric ozone: An observation-based review. *Elem Sci Anth*, 2, p.000029. DOI: http://doi.org/10.12952/journal.elementa.000029, 2014.

Cronin, T., Gemery, L., Briggs, W., Jakobsson, M., Polyak, L. and Brouwers, E., Quaternary Sea-ice history in the Arctic Ocean based on a new Ostracode sea-ice proxy, *Quaternary Science Reviews*, 29(25), 3415-3429, 2010.

305   Cuevas, C. A., Maffezzoli, N., Corella, J. P., Spolaor, A., Vallelonga, P., Kjær, H. A., Simonsen, M., Winstrup, M., Vinther, B. and Horvat C, Rapid increase in atmospheric iodine levels in the North Atlantic since the mid-20th century, *Nature communications*, 9 (1), 1452, 2018.

Dansgaard, W., Johnsen, S., A flow model and a time scale for the ice core from Camp Century, Greenland, *Journal of Glaciology*, 8(53), 215-223, 1969.

310   W. H. Organization, Iodine status worldwide: WHO global database on iodine deficiency. B. De Benoist, M. Andersson, I. M. Egli, T. El Bahi, H. Allen, Eds, 2004.

Gálvez, Ó., Baeza-Romero, M. T., Sanz, M. and Saiz-Lopez, A., Photolysis of frozen iodate salts as a source of active iodine in the polar environment. *Atmospheric Chemistry and* Physics 16, 12703-12713, 2016.

Hansson, M. E., The Renland ice core. A Northern Hemisphere record of aerosol composition over 120,000 years.
315   *Tellus B: Chemical and Physical Meteorology*, *46*(5), 390-418, 1994.

Hossaini, R., Chipperfield, M., Montzka, S., Rap, A., Dhomse, S.and Feng, W., Efficiency of short-lived halogens at influencing climate through depletion of stratospheric ozone, *Nature Geoscience*, *8*(3), 186, 2015.

Jennings, A. E., Knudsen, K. L., Hald, M., Hansen, C. V. and Andrews, J. T. , A mid-Holocene shift in Arctic sea-ice variability on the East Greenland Shelf, *The Holocene*, *12*(1), 49-58, 2002.

320   Kaufman, D. S., Ager, T. A., Anderson, N. J., Anderson, P. M., Andrews, J. T., Bartlein, P. J., Brubaker, L. B., Coats, L. L., Cwynar, L. C. and Duvall, M. L., Holocene thermal maximum in the western Arctic (0–180 W), *Quaternary Science Reviews*, *23*(5-6), 529-560, 2004.

Kim, K., Yabushita, A., Okumura, M., Saiz-Lopez, A., Cuevas, C. A., Blaszczak-Boxe, C. S., Min, D., W. Yoon, H.-I. and Choi, W., Production of molecular iodine and tri-iodide in the frozen solution of iodide: implication for polar atmosphere,
325   *Environmental science & technology*, *50*(3), 1280-1287, 2016.

Koç, N., Jansen, E., and Haflidason, H., Paleoceanographic reconstructions of surface ocean conditions in the Greenland, Iceland and Norwegian seas through the last 14 ka based on diatoms, *Quaternary Science Reviews*, *12*(2), 115-140, 1993.

Kolling, H. Stein, M., R., Fahl, K., Perner, K. and Moros M., Short-term variability in late Holocene sea ice cover on
330   the East Greenland Shelf and its driving mechanisms, *Palaeogeography, Palaeoclimatology, Palaeoecology*, *485*, 336-350, 2017.

Kristjánsdóttir, G. B., Moros, M., Andrews, J. T. and Jennings, A. E., Holocene Mg/Ca, alkenones, and light stable isotope measurements on the outer North Iceland shelf (MD99-2269): A comparison with other multi-proxy data and sub-division of the Holocene, *The Holocene*, *27*(1), 52-62, 2017.

335   Legrand, M., McConnell, J. R., Preunkert, S., Arienzo, M., Chellman, N., Gleason, K., Sherwen, T., Evans, M. J. and Carpenter, L. J., Alpine ice evidence of a three-fold increase in atmospheric iodine deposition since 1950 in Europe due to increasing oceanic emissions, *Proceedings of the National Academy of Sciences*, *115*(48), 12136-12141, 2018.

MacDonald, S., Gómez Martín, J., Chance, R., Warriner, S., Saiz-Lopez, A., Carpenter, L. and Plane, J., A laboratory characterisation of inorganic iodine emissions from the sea surface: dependence on oceanic variables and parameterisation for
340   global modelling, *Atmospheric Chemistry and Physics*, *14*(11), 5841-5852, 2014.

McFiggans, G., Plane, J. M. C., Allan, B. J., Carpenter, L. J., Coe, H., and O'Dowd, C., A modeling study of iodine chemistry in the marine boundary layer, J Geophys. Res-Atmos., 105, 14 371-14 385, doi:10.1029/1999JD901187, 2000.

Maffezzoli, N., Vallelonga, P., Edwards, R., Saiz-Lopez, A., Turetta, C., Kjær, H. A., Barbante, C., Vinther, B. and Spolaor, A., 120,000 year record of sea ice in the North Atlantic, *Climate of the Past Discussions*, https://doi.org/10.5194/cp-
345   2018-80, 2018.

Mahajan, A., Sorribas, M., Gómez Martín, J., MacDonald, S., Gil, M., Plane, J. and Saiz-Lopez A., Concurrent observations of atomic iodine, molecular iodine and ultrafine particles in a coastal environment, *Atmospheric Chemistry and Physics*, *11*(6), 2545-2555, 2011.

350   Mahajan, A., Gómez Martín, J., Hay, T., Royer, S.-J., Yvon-Lewis, S., Liu, Y., Hu, L., Prados-Roman, C., Ordóñez, C. and Plane, J., Latitudinal distribution of reactive iodine in the Eastern Pacific and its link to open ocean sources, *Atmospheric Chemistry and Physics*, *12*(23), 11609-11617, 2012.

Mayewski, P.A., Rohling, E.E., Curt Stager, J., Karlén, W., Maasch, K.A., David Meeker, L., Meyerson, E.A., Gasse, F., van Kreveld, S., Holmgren, K., Lee-Thorp, J., Rosqvist, G., Rack, F., Staubwasser, M., Schneider, R.R. and Steig, E.J., Holocene climate variability. *Quaternary Research* 62(3), 243-255, 2004.

355   Müller, J., Werner, K., Stein, R., Fahl, K., Moros, M. and Jansen, E., Holocene cooling culminates in sea ice oscillations in Fram Strait, *Quaternary Science Reviews*, *47*, 1-14, 2012.

Nesje, A., and Dahl, S. O., Lateglacial and Holocene glacier fluctuations and climate variations in western Norway: a review, *Quaternary Science Reviews*, *12*(4), 255-261, 1993.

O' Dowd, C. D., Jimenez, J. L., Bahreini, R., Flagan, R. C., Seinfeld, J. H., Hämeri, K., Pirjola, L., Kulmala, M.,
360   Jennings, S. G. and Hoffmann, T., Marine aerosol formation from biogenic iodine emissions, *Nature*, *417*(6889), 632, 2002.

Overland, J. E., and Wang, M., When will the summer Arctic be nearly sea ice free?, *Geophysical Research Letters*, *40*(10), 2097-2101, 2013

Prados-Roman, C., Cuevas, C., Fernandez, R. D., Kinnison, D., Lamarque, J.-F. and Saiz-Lopez, A., A negative feedback between anthropogenic ozone pollution and enhanced ocean emissions of iodine, *Atmospheric Chemistry and*
365   *Physics*, *15*(4), 2215-2224, 2015

Rienecker, M. M., Suarez, M. J., Gelaro, R., Todling, R., Bacmeister, J., Liu, E., Bosilovich, M. G., Schubert, S. D., Takacs, L. and Kim, G.-K., MERRA: NASA's modern-era retrospective analysis for research and applications, *Journal of climate*, *24*(14), 3624-3648, 2011.

Roscoe, H. K., Jones, A. E., Brough, N., Weller, R., Saiz-Lopez, A., Mahajan, A. S., Schoenhardt, A., Burrows, J. P.,
370   and Fleming, Z. L., Particles and iodine compounds in coastal Antarctica, *Journal of Geophysical Research: Atmospheres*, *120*(14), 7144-7156, 2015.

Saiz-Lopez, A., and von Glasow, R., Reactive halogen chemistry in the troposphere, *Chemical Society Reviews*, *41*(19), 6448-6472, 2012.

Saiz-Lopez, A., Blaszczak-Boxe, C.S. and Carpenter, L., A mechanism for biologically induced iodine emissions
375   from sea ice, *Atmospheric Chemistry and Physics*, *15*(17), 9731-9746, 2015.

Saiz-Lopez, A., Fernandez, R., Ordóñez, C.,, Kinnison, D. Gómez Martín, J., Lamarque, J.-F. and Tilmes, S., Iodine chemistry in the troposphere and its effect on ozone, *Atmospheric Chemistry and Physics*, *14*(23), 13119-13143, 2014.

Saiz-Lopez, A., Plane, J. M., Baker, A. R., Carpenter, L. J., von Glasow, R., Gómez Martín, J. C., McFiggans, G. and Saunders, R. W., Atmospheric chemistry of iodine, *Chemical reviews*, *112*(3), 1773-1804, 2012.

380   Saiz-Lopez, A., Plane, J., Mahajan, A., Anderson, P., Bauguitte, S.-B., Jones, A., Roscoe, H., Salmon, R., Bloss, W., and Lee, J., On the vertical distribution of boundary layer halogens over coastal Antarctica: implications for O3, HOx, NOx and the Hg lifetime, *Atmospheric Chemistry and Physics*, *8*(4), 887-900, 2008.

Saiz-Lopez, A., Lamarque, J.-F., Kinnison, D., Tilmes, S., Ordóñez, C., Orlando, J., Conley, A., Plane, J., Mahajan, A. and Sousa Santos, G., Estimating the climate significance of halogen-driven ozone loss in the tropical marine troposphere,
385   *Atmospheric Chemistry and Physics*, *12*(9), 3939-3949, 2012.

Sherwen, T., Schmidt, J. A., Evans, M. J., Carpenter, L. J., Großmann, K., Eastham, S. D., Jacob, D. J., Dix, B., Koenig, T. K., Sinreich, R., Ortega, I., Volkamer, R., Saiz-Lopez, A., Prados-Roman, C., Mahajan, A. S., and Ordóñez, C., Global impacts of tropospheric halogens (Cl, Br, I) on oxidants and composition in GEOS-Chem, *Atmos. Chem. Phys.*, 16, 12239-12271, 2016.

390   Sherwen, T., Evans, M. J., Carpenter, L. J., Schmidt, J. A., and Mickley, L. J., Halogen chemistry reduces tropospheric O3 radiative forcing, *Atmos. Chem. Phys.*, 17, 1557-1569, 2017.

Sipilä, M., Sarnela, N., Jokinen, T., Henschel, H., Junninen, H., Kontkanen, J., Richters, S., Kangasluoma, J., Franchin, A. and Peräkylä, O., Molecular-scale evidence of aerosol particle formation via sequential addition of HIO3, *Nature*, *537*(7621), 532, 2016.

395   Ślubowska-Woldengen, M., Koç, N., Rasmussen, T. L., Klitgaard-Kristensen, D., Hald, M. and Jennings, A. E., Time-slice reconstructions of ocean circulation changes on the continental shelf in the Nordic and Barents Seas during the last 16,000 cal yr BP, *Quaternary Science Reviews*, *27*(15), 1476-1492, 2008.

Solignac, S., Giraudeau, J. and de Vernal, A., Holocene sea surface conditions in the western North Atlantic: spatial and temporal heterogeneities, Paleoceanography, 21(2). PA2004, doi:10.1029/2005PA001175, 2006.

400 Solomina, O. N., Bradley, R. S., Hodgson, D. A., Ivy-Ochs, S., Jomelli, V., Mackintosh, A. N., Nesje, A., Owen, L. A., Wanner, H. and Wiles, G. C., Holocene glacier fluctuations, *Quaternary Science Reviews*, *111*, 9-34, 2015.

Spolaor, A., Vallelonga, P., Plane, J., Kehrwald, N., Gabrieli, J., Varin, C., Turetta, C., Cozzi, G., Kumar, R. and Boutron, C., Halogen species record Antarctic sea ice extent over glacial–interglacial periods, *Atmospheric Chemistry and Physics*, *13*(13), 6623-6635, 2013.

405 Spolaor, A., Opel, T., McConnell, J., Maselli, O., Spreen, G., Varin, C., Kirchgeorg, T., Fritzsche, D., Saiz-Lopez, A. and Vallelonga, P., Halogen-based reconstruction of Russian Arctic sea ice area from the Akademii Nauk ice core (Severnaya Zemlya). *The Cryosphere* 10, 245-256, 2016.

Telesinski, M., Spielhagen, R. F. and Bauch, H. A., Water mass evolution of the Greenland Sea since late glacial times, *Climate of the Past*, *10*, 123-136, 2014

410 Telesiński, M., Bauch, H. A., Spielhagen, R. F. and Kandiano E. S., Evolution of the central Nordic Seas over the last 20 thousand years, *Quaternary Science Reviews*, *121*, 98-109, 2015.

Telesiński, M., Spielhagen, M., R. F. and Lind, E. M., A high-resolution L ateglacial and H olocene palaeoceanographic record from the G reenland S ea, *Boreas*, *43*(2), 273-285, 2014

Vallelonga, P., Maffezzoli, N., Moy, A. D., Curran, M. A. J., Vance, T. R., Edwards, R., Hughes, G., Barker, E., 415 Spreen, G., Saiz-Lopez, A., Corella, J. P., Cuevas, C. A., and Spolaor, A.: Sea-ice-related halogen enrichment at Law Dome, coastal East Antarctica, Clim. Past, 13, 171-184, https://doi.org/10.5194/cp-13-171-2017, 2017.

Vare, L. L., Masse, G., Gregory, T. R., Smart, C. W. and Belt, S. T., Sea ice variations in the central Canadian Arctic Archipelago during the Holocene, *Quaternary Science Reviews*, *28*(13-14), 1354-1366, 2009.

Vinther, B. M., Clausen, H. B., Johnsen, S. J., Rasmussen, S. O., Andersen, K. K., Buchardt, S. L., Dahl-Jensen, D., 420 Seierstad, I. K. , Siggaard-Andersen, M. L. and Steffensen, J. P., A synchronized dating of three Greenland ice cores throughout the Holocene, *Journal of Geophysical Research: Atmospheres*, *111*(D13), 2006.

Vinther, B. M., Buchardt, S. L., Clausen, H. B., Dahl-Jensen, D., Johnsen, S. J., Fisher, D., Koerner, R., Raynaud, D., Lipenkov, V. and Andersen, K., Holocene thinning of the Greenland ice sheet, *Nature*, *461*(7262), 385, 2009.

Volkman, J. K., Barrett, S. M., Blackburn, S. I., Mansour, M. P., Sikes, E. L. and Gelin, F., Microalgal biomarkers: 425 a review of recent research developments, *Organic Geochemistry*, *29*(5-7), 1163-1179, 1998.

Volkmann, R., Planktic foraminifer ecology and stable isotope geochemistry in the Arctic Ocean: implications from water column and sediment surface studies for quantitative reconstructions of oceanic parameters= Ökologie planktischer Foraminiferen und stabile Isotope im Arktischen Ozean: Anwendbarkeit für die quantitative Rekonstruktion von ozeanischen Parametern, *Berichte zur Polarforschung (Reports on Polar Research)*, *361*, 2000.

430 Volz, A. and Kley, D., Evaluation of the Montsouris series of ozone measurements made in the nineteenth century, *Nature*, *332*(6161), 240, 1988.

Wegner, C., Bennett, K. E., de Vernal, A,. Forwick, M., Fritz, M., Heikkilä, M., Łącka, M., Lantuit, H., Laska, M., and Moskalik, M., Variability in transport of terrigenous material on the shelves and the deep Arctic Ocean during the Holocene, *Polar Research*, *34*(1), 24964, 2015.

435 Werner, K., Spielhagen, R. F., Bauch, D., Hass, H. C. and Kandiano, E., Atlantic Water advection versus sea-ice advances in the eastern Fram Strait during the last 9 ka: Multiproxy evidence for a two-phase Holocene, *Paleoceanography*, *28*(2), 283-295, 2013.

Werner, K., Müller, J., Husum, K., Spielhagen, R. F., Kandiano, E. S. and Polyak, L., Holocene sea subsurface and surface water masses in the Fram Strait–Comparisons of temperature and sea-ice reconstructions, *Quaternary Science Reviews*, 440 *147*, 194-209, 2016.

Winstrup, M., Svensson, A., Rasmussen, S. O., Winther, O., Steig, E. and Axelrod, A., An automated approach for annual layer counting in ice cores, *Climate of the Past*, *8*(6), 1881-1895, 2012.

Xiao, X., Zhao, M., Knudsen, K. L., Sha, L., Eiríksson, J., Gudmundsdóttir, E., Jiang, H. and Guo, Z., Deglacial and Holocene sea–ice variability north of Iceland and response to ocean circulation changes, *Earth and Planetary Science Letters*, 445 *472*, 14-24, 2017.
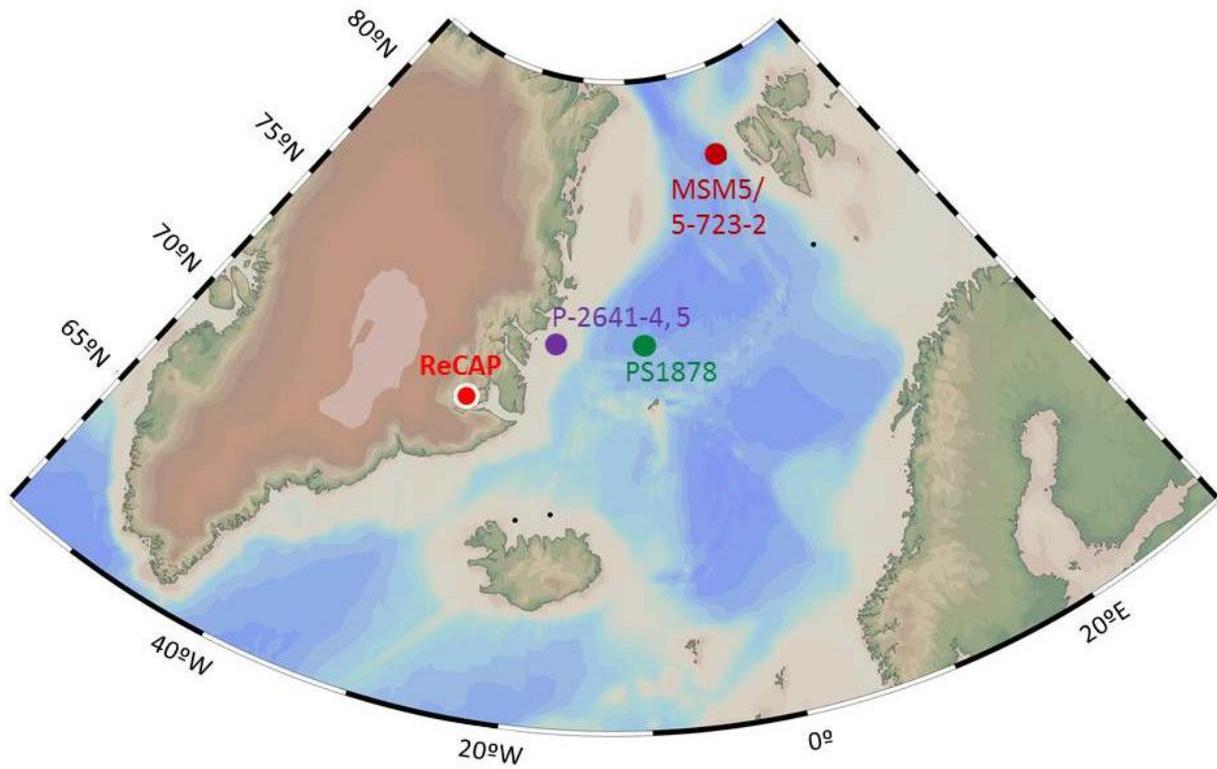
Fig. 1: Location of the ReCAP ice core (red) and other marine paleoceanographic archives in the Nordic Seas discussed in the text.
For references of the paleoenvironmental proxies from the displayed sediment cores, please refer to the text and Fig. 2 caption.
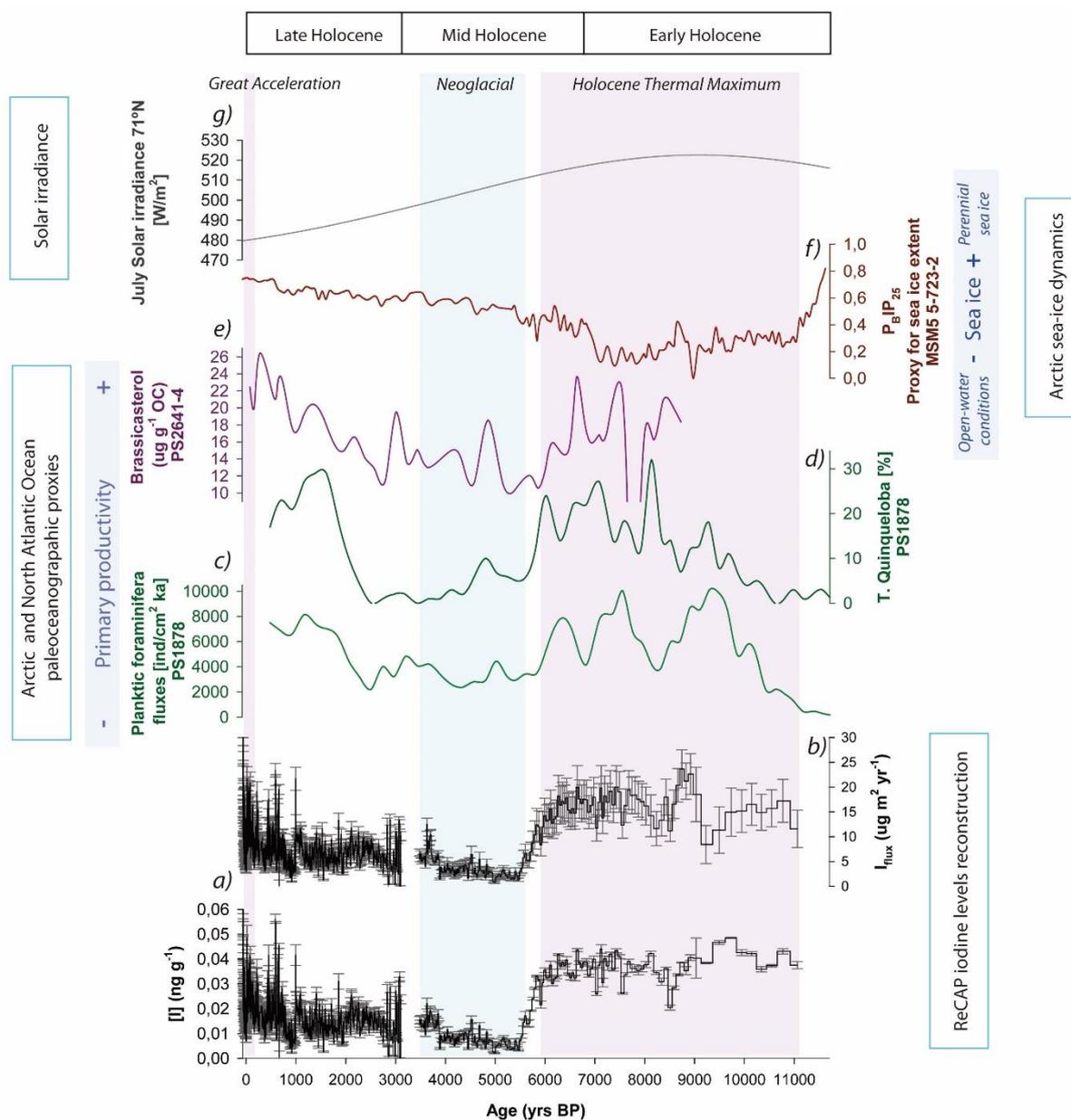
Fig. 2: Holocene iodine concentration and fluxes evolution from the ReCAP ice core and primary productivity and sea-ice cover proxies from the Nordic seas. From bottom to top: **a)** Iodine concentrations (1σ, experimental uncertainties) and **b)** fluxes (1σ, propagated from the concentration and accumulation rate uncertainties) (N=1050); **c)** and **d)** Planktic foraminifera and *T. quinqueloba* (core PS1878) (*M Telesiński et al.*, 2015), **e)** *Brassicasterol* (core PS2641-4) (*Müller et al.*, 2012); **f)** Sea-ice cover (core MSM5 5/723-2) (*Werner et al.*, 2013; *Werner et al.*, 2016); **g)** 71°N July solar irradiance. Color boxes indicate the Holocene main climatic periods mentioned in the text; pink boxes indicate warmer phases while blue boxes indicate colder intervals.

14
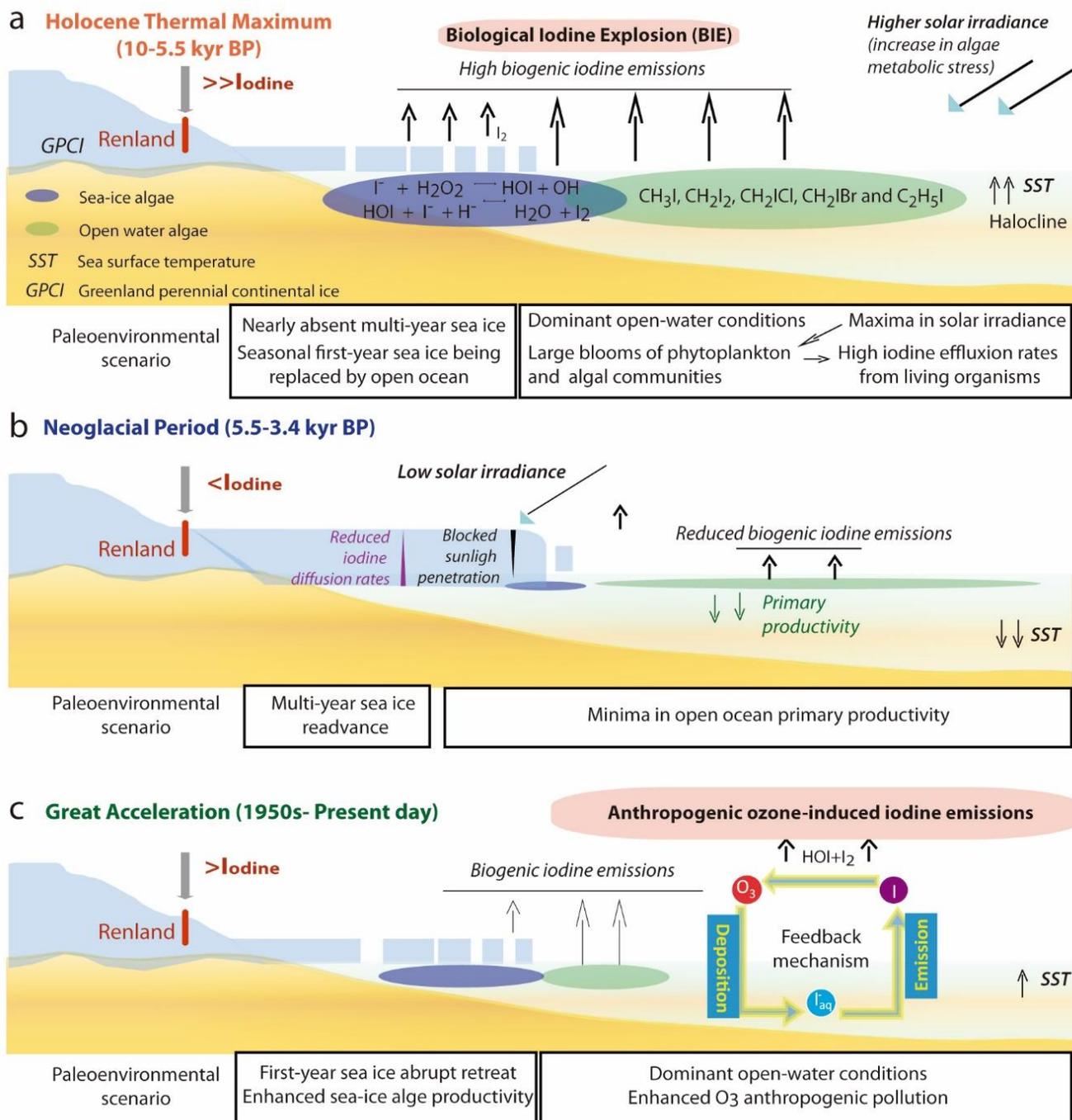
Fig. 3: Schematic diagram showing the coupled ocean-atmosphere iodine biogeochemical cycle throughout the Holocene. (a) Holocene Thermal Maximum. (b) Neoglacial period. (c) Great Acceleration.